

# THE SPS TESTS OF THE HL-LHC CRAB CAVITIES

R. Calaga, O. Capatina, G. Vandoni  
 CERN, Geneva, Switzerland

## Abstract

Two superconducting crab cavities in the framework of the High Luminosity (HL-LHC) LHC were built to test for the first time with proton beams in the Super Proton Synchrotron (SPS) at CERN. These tests will address the operation of the crab cavities in a high current and high energy proton machine through the full energy cycle with a primary focus on cavity transparency, performance and stability, failure modes and long term effects on proton beams. An overview of the SPS cryomodule development towards the SPS tests along with the first test results are presented.

## INTRODUCTION

After careful analysis of the use of crab cavities for HL-LHC, it was decided to first test the superconducting technology in the CERN-SPS with high energy and high current proton beams [1]. These tests were deemed an essential step with regard to differences between electron and proton beams. During the design studies it became clear that mastering cavity operation in the complex LHC energy cycle and to precisely control the cavity fields over long runs are paramount. The beam test in the SPS will allow the demonstration of crab cavity transparency, effects of RF non-linearity, cavity alignment, RF power transients, beam stability, HOM power and other relevant aspects required for stable operation in the LHC.

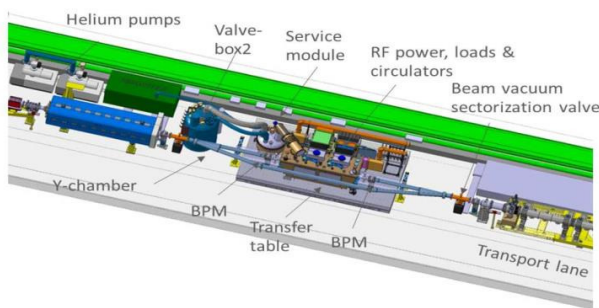


Figure 1: Layout of the crab cavity installation zone in the SPS-LSS6.

The crab cavity cryomodule [2] is located in the SPS LSS6 (Figure 1), a region dedicated to beam extraction to the LHC. The module is positioned on a motorized transfer table. Two Y-shaped vacuum chambers ensure the vacuum line continuity, allowing to keep the cavities on a by-pass of the main beam-line during regular SPS operation and to move them into the beam path during dedicated experimental runs.

The entrance diameter of the crab cavities is smaller than the aperture needed for beam extraction to the LHC. Vacuum valves allow to isolate the beam line by-pass, to guarantee machine protection against failure of the prototype module. The main parameters of the SPS machine in LSS6 are listed in Table 1.

Table 1: SPS Parameters for Crab Cavity Beam Tests

	Unit	Value
Energy	[GeV]	26-270
Bunch intensity	$[\times 10^{11}]$	0.01-1.0
Main RF frequency	[MHz]	200.39
Crab Frequency	[MHz]	$400.6 \pm 0.2$
Bunch length	[ns]	1.0-2.0
Long. position	[m]	6312.72, 6313.32
Total bypass length	[m]	10
$\beta_x, \beta_y, D_x$	[m]	40, 80, -0.5
$Q_x, Q_y$	-	26.12, 26.18
Crab cavity aperture	[mm]	84

## PERFORMANCE & LIMITATIONS

A minimum of 1 MV/cavity was set as a criterion for installation in the SPS for beam tests. From the results of the vertical tests performed on the dressed cavities, the stable operational voltage of 2.5 MV per cavity is within reach. The cause of the voltage degradation of the dressed cavity with respect to the bare cavity - which reached 5 MV - is not yet understood and RF testing with a prototype cavity and HOMs is ongoing. During warm-up after vertical test, a large leak opened on two out of the three HOM feed-throughs. The HOM feed-throughs were replaced by a back-up model of consolidated design, but with lower power capabilities ( $\sim 200$  W), while further studies are done to understand the reason of the fault. The power limitation does not impact the SPS beam tests, as the HOM power is not expected to exceed 200 W in the SPS at maximum current. A redesign of the higher power feed-throughs is under way, with the aim to validate their robustness during thermal cycles for HL-LHC cavities [3].

A complete cool-down of cryomodule was performed in the SM18 test facility prior to the installation into the SPS. Two cool-down cycles were performed. These proved the mechanical and cryogenic performance in terms of intercavity movements and pipe sizing. Static heat load of the cryomodule was measured with evaporative methods and determined to be  $\sim 18$  W. This value is comparable with the 17 W inferred from simulations of the cryomodule's

Content from this work may be used under the terms of the CC BY 3.0 licence (© 2018). Any distribution of this work must maintain attribution to the author(s), title of the work, publisher, and DOI.

thermal performance [4]. A thorough alignment campaign was carried out to measure the inter-cavity alignment during the cryomodule assembly and cool-down [5]. The final horizontal and vertical alignment of the cavities was determined to be inferior to  $130\ \mu\text{m}$ , in both the horizontal and vertical plane. To span the overall  $\pm 150\ \text{kHz}$  of the SPS energy cycles, a complete tuning cycle was successfully demonstrated. Hysteresis was observed to be very small, with tuning resolution below  $1\ \text{Hz}$  [6]. A 2K testing campaign to measure comprehensive higher order modes (HOM) was also carried out and compared to simulations, with good agreement [7].

RF conditioning was performed up to  $600\ \text{W}$  ( $\sim 0.8\text{MV}$ ), due to lack of water cooling of the high power coupler in the test setup. Partial conditioning was performed with  $4\ \text{ms}$  pulses with a  $10\%$  duty cycle up to maximum power, showing signs of a long tail in vacuum activity [3]. The full RF conditioning will be performed directly in the SPS up to the maximum safe voltage. The RF controls were subsequently used to drive the cavities; frequency locking and feedback loops were demonstrated to operate as expected [8]. RF phase noise measurements were also performed, showing that the measured noise from the cavity closely followed the reference oscillator [8]. Improvements on the LLRF electronics will therefore become necessary for the HL-LHC, which requires very low phase noise to limit emittance growth.

## INFRASTRUCTURE

In the SPS (Figure 2), two vacuum sector valves enclose a new vacuum sector, comprising two Y-shaped vacuum chambers articulated by mechanical bellows, the circulating beam line and the beam bypass with the cryomodule. All beam-pipes in this vacuum sector are coated with a thin film of amorphous carbon, to reduce secondary electron yield and consequently mitigate electron cloud [9]. The cryomodule itself is further nested in a separate vacuum sector by two additional vacuum valves, separating cold from conventional beam vacuum. Two dedicated beam position monitors (BPM) are included in this smaller vacuum sector on either side of the cryomodule, providing independent amplitude and beam phase signals for the low-level RF control system. All connecting vacuum chambers have been carefully designed to limit impedance.

The remotely operated table, designed by AVS Spain [10], ensures reproducible transfer of the cryomodule in beam and in parking in less than 10 minutes, with a  $510\ \text{mm}$  translation and a positioning precision of  $4\ \mu\text{m}$ , as checked by Frequency Scanning Interferometry (FSI) [11]. Besides the cryomodule, the table carries passive RF circulators and loads, a cryogenic service module and the supports of the articulated vacuum chambers, for a total load reaching 15 tons. The table position is monitored by LVDTs and by the stepper motor's resolvers, the latter calibrated independently with the FSI system. The table end-switches provide double-redundant interlocking

for the SPS beam. Table movement is itself interlocked by the vacuum sector valves, which need to be closed to mitigate the risk of beam vacuum rupture while moving the cold cryomodule.

A new cryogenic system, including a mobile refrigerator, provides the cooling capacity in the SPS [12]. The warm compressor unit, located at the surface (see Figure 3), is connected to the cold-box underground by two warm lines for high and low pressure gas. Integration is studied to allow for removal and relocation of both the warm equipment and the cold-box, with the connecting pipework and cabling remaining in situ. The cold-box refrigeration capacity is boosted with a first stage of liquid nitrogen fed heat exchanger. Liquid nitrogen is routed to the cold-box from a surface tank via a  $50\text{m}$  long vertical transfer line. With liquid nitrogen boosting, the liquefaction capacity of the cold-box attains  $7\ \text{g/s}$ . A  $80\ \text{m}$  long horizontal transfer line connects the cold-box to the cryomodule. Refrigeration to  $2\text{K}$  is obtained with 2 large pumping units, providing a total cooling capacity of  $3.5\ \text{g/s}$  at  $30\ \text{mbar}$  (saturation at  $2\ \text{K}$ ). The capacity of the new cold box is thus fully responding to specification, which was to cover crab cavity static and dynamic heat losses including a contingency factor of 1.5 (at least  $48\ \text{W}$  at  $2\ \text{K}$ , equivalent to  $2\ \text{g/s}$ ).

Due to limited space underground, the two IOT-type (Inductive Output Tube) RF amplifiers, providing the  $60\ \text{kW}$  cw power, were installed at the surface and power routed to the cryomodule via coaxial lines. Two V-shaped RF coaxial transmission lines with rotating connections provide the required flexibility to follow the table movement [3]. The surface equipment is completed by a Faraday cage, shielding the Low Level RF equipment from the nearby IOTs. This configuration allows the validation of the cavity control with long loop delay time between the LLRF and the cavities of the order  $2\ \mu\text{s}$  or more.

## BEAM TEST PREPARATIONS

Four major systems including the cryomodule itself will be commissioned during the beam test phase.

Cavity and cryomodule: Performance studies will include stability, RF gymnastics and beam induced transients. Special attention will be given to the transparency using the two cavities in counter-phase during operation.

High power amplifiers (IOTs): The overall performance study of the RF transients, to reliably provide the required  $40\ \text{kW}$  cw and up to  $60\text{-}80\ \text{kW}$  peak; the robustness in beam of the high power feed-throughs, input coupler and the HOMs.

Cryogenic system: Tests will validate proper dimensioning of the  $2\text{K}$  sub-atmospheric cryogenics under dynamic heat load with beam, as well as its stability in time.

Vacuum system: The crab vacuum system will be tested, including the performance impact on superconducting cavities of the amorphous carbon coated beam pipes.

The experimental program and the technical validation in the SPS is split in four phases: RF beam synchronization,



Figure 2: Surface and tunnel installation of the cryogenic, mechanical and RF infrastructure to support the crab cavity testing in the SPS-LSS6 region.

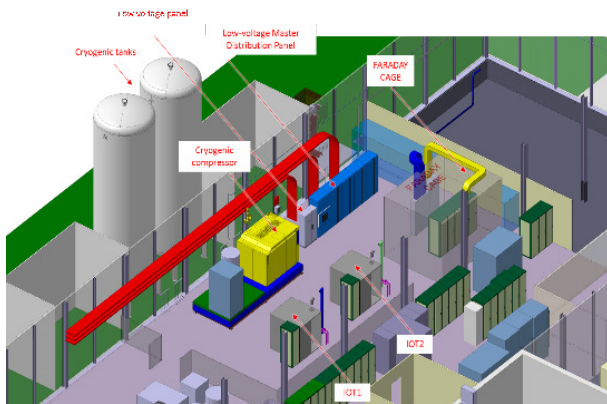


Figure 3: Schematic of the surface installation of the cryogenic, mechanical and RF infrastructure.

cavity transparency studies, performance and stability, high intensity operation.

The beam tests in the SPS will provide the first demonstration of deflecting cavity field with proton beams, with active control of cavity field in amplitude and phase. Following the verification of operational frequency, tuning sensitivity, input power overhead and HOM signals, it will be possible to define the comprehensive operational cycle for the LHC. Since the mechanical tuner of the crab cavities cannot follow the fast energy ramp of the SPS, the injection of the beam into the SPS will be performed with the cavities synchronized to the accelerating RF system and a small voltage. At energies above injection, the frequency is tuned to a fixed value at that energy and the main RF is re-synchronized.

Operation w/o crab cavity action, will be studied for energies between 26 GeV to 450 GeV, by either counter-phasing the two cavities or by appropriate detuning (to parking position). The residual leakage and the adiabatic change from a transparent mode to a fully crabbed mode will be comprehensively tested, to validate the RF gymnastics needed for reliable operation in the HL-LHC.

Beam measurements for orbit centering, crab dispersive orbit and bunch rotation, will also be carried out. Other aspects such as the demonstration of non-correlated operation of two cavities in a common CM, triggering a quench in one cavity without inducing a quench in the other, implementation of interlock hierarchy and verification of machine protection aspects and functioning of slow and fast

interlocks, will also be studied. It will be important to test HOM coupler operation with high beam currents, different filling schemes and associated power levels. The characterization of the HOM power and its distribution between the different couplers is essential to validate the damping and power extraction. Although beam stability due to the impedance of the crab cavity is not expected to be an issue in the SPS, studies to investigate the onset of the coupled bunch instabilities due to the fundamental mode with feedback gain reduction is useful for scaling impedance effects to the HL-LHC.

The measurement of emittance growth induced by the crab cavities and the study of general long term behavior with proton beams are also a necessary objective. The effect of the amplitude and phase noise from the crab cavity on the beam and the resulting emittance growth are another concern for using crab cavities in long physics fills. Several experimental sessions were carried out to measure the natural emittance growth to determine the long term behavior without crab cavities since 2009. A set of beam and machine parameters at a beam energy of 270 GeV shows consistent emittance growth of approximately  $0.3 - 0.5 \mu\text{m/hr}$  [13].

## ACKNOWLEDGMENTS

We would like to express our immense gratitude to entire HL-LHC crab cavity team with a special emphasis to the members of BE, EN and TE departments at CERN as well as the UK and US collaboration for their valuable contributions to the project.

## REFERENCES

- [1] R. Calaga, "Crab cavities for the LHC upgrade" in *Proc. Chamonix 2012 Workshop on LHC performance*, <https://espace.cern.ch/acc-tec-sector/Chamonix/Chamx2012/book/ProceedingsAll.pdf>.
- [2] M. Garlasche et al., "Assembly of the DQW crab-cavity cryomodule for SPS test", presented at the 9th Int. Particle Accelerator Conf. (IPAC18), Vancouver, Canada, Apr.-May 2018, paper WEPMF078.
- [3] E. Montesinos et al., private communication, Jan. 2018.
- [4] F. Carra et al., "Thermal performance of the DQW crab-cavity cryomodule for HL-LHC", July 2017, unpublished.

- [5] H. Mainaud Durand et al., "Frequency Scanning Interferometry as new solution for on-line position monitoring inside a cryostat", presented at the 9th Int. Particle Accelerator Conf. (IPAC18), Vancouver, Canada, Apr.–May 2018, paper WEPAF068.
- [6] J. Swieszek, K. Artoos, J. Mitchell, private communication, Nov. 2017.
- [7] J. Mitchell et al., "Simulation and measurements of crab-cavity HOMs and HOM couplers for HL-LHC", in *Proc. 18th International Conference on RF Superconductivity, SRF2017*, Lanzhou, China, July 2017, paper THPB059, pp. 881–885, <https://doi.org/10.18429/JACoW-SRF2017-THPB059>
- [8] P. Baudrenghien et al., private communication, Dec. 2017.
- [9] C Yin Vallgren et al., "Amorphous carbon coatings for mitigation of electron cloud in the CERN SPS", in *Proc. IPAC'10*, Kyoto, Japan, May 2010, paper TUPD048, pp. 2033–2035.
- [10] AVS, Spain, "Technical and Construction folder of the crab-cavity transfer table for the CERN SPS", unpublished, Jan. 2018.
- [11] M. Sosin et al., "Position monitoring system for HL-LHC crab cavities" in *Proc. IPAC'16*, Busan, Korea, May 2016, paper WEPOR018, pp. 2704–2706, doi:10.18429/JACoW-IPAC2016-WEPOR018.
- [12] S. Claudet et al., private communication, Oct. 2018.
- [13] F. Antoniou et al., "Emittance growth studies in coasting beams in the SPS", presented at the 9th Int. Particle Accelerator Conf. (IPAC18), Vancouver, Canada, Apr.–May 2018, paper MOPMF061.